# Global Optimization of a Hybrid Waste Tire and Natural Gas Feedstock Polygeneration System

Avinash S.R. Subramanian[a], Truls Gundersen[a], Paul I. Barton[b], Thomas A. Adams II[c]

[a] *Department of Energy and Process Engineering, Norwegian University of Science and Technology (NTNU), Kolbjørn Hejes vei 1B, NO-7491, Trondheim, Norway.*
[b] *Process Systems Engineering Laboratory, Department of Chemical Engineering, Massachusetts Institute of Technology, 77 Massachusetts Avenue, Cambridge, Massachusetts 02139, United States.*
[c] *Department of Chemical Engineering, McMaster University, 1280 Main St. W, Hamilton, ON, Canada, L8S 4L7.*

**Abstract**

The globally optimal design and operation of a process that converts a hybrid waste tire and natural gas feedstock to multiple products (such as electricity, methanol, dimethyl ether, olefins, and liquefied natural gas) as part of a polygeneration scheme is presented. A three-step methodology is followed: First, rigorous process models for the mass and energy balance calculations are implemented; next, these models are sampled to generate data that are used to fit surrogate models which take the form of algebraic equations relating input and output variables for each process section; lastly, a Mixed-Integer Nonlinear Program that maximizes net present value is formulated using the recently developed GOSSIP software and solved with the linked ANTIGONE solver. The optimal product portfolio under a variety of market and policy scenarios is presented for two cases: Without and with waste tire tipping fees of 100 \$/tonne. Furthermore, the synergies between the waste tire and natural gas feedstocks are investigated. The optimal product portfolio is found to be highly sensitive to prevailing market conditions thus motivating future work on design under uncertainty of flexible polygeneration processes that are able to change operating conditions in response to varying prices.

*Keywords:* Polygeneration system, Waste-to-Energy, Gasification, Global optimization, $CO_2$ capture, Waste Tire, Natural Gas

## 1. Introduction

Polygeneration involves the production of multiple products such as a mix of electricity, fuels (gasoline, diesel, synthetic natural gas, hydrogen) and chemicals (methanol, dimethyl ether, olefins, acetic acid) in the same location. Thus, part of the motivation for designing polygeneration plants is to provide added financial security arising from this diversification [1]. An additional strategy is to use multiple complementary feedstocks, such as a mix of coal, natural gas, solid wastes, biomass, uranium etc., in order to enable tighter integration and exploitation of certain synergies [2]. For instance, Adams and Barton proposed a novel polygeneration process in which an exothermic coal gasifier is heat integrated with an endothermic natural gas reforming process [3]. This concept is extended to utilize carbonless heat generated in a modular helium nuclear reactor [4, 5]. Further improvement in efficiency is derived by generating syngas of different quality from each feed followed by blending these streams in order to provide the correct composition for later product synthesis instead of implementing exergetically expensive syngas upgrading or downgrading steps. Including an alternative feedstock (such as waste tire [6, 7], plastics, municipal solid waste [8] or petcoke [9, 10]) may also allow energy companies to lower their overall environmental impact while mitigating energy security concerns. A final advantage of hybrid feedstock polygeneration systems is that they may have higher profitability as a result of economies of scale if certain equipment such as cleaning units are shared [3, 11]. Reviews of polygeneration systems are presented by Adams and Ghouse [12], Jana et al. [13] and Murugan and Horak [14].

In our previous work [6, 7], we studied the conversion of waste tire as a single feedstock. We used the gasification process as a means to recover both valuable material and energy from the tire. This stands in contrast to current approaches of tire management such as incineration (where only energy is recovered), grinding for use in civil engineering applications such as on playground surfaces (where only material is recovered) or stockpiling (where neither is recovered). We investigated both the use of rotary kiln gasifiers [6] and Entrained Flow (EF) gasifiers (with a similar gasifier design to that used commercially for coal gasification) and provided a brief account of advantages and disadvantages of each [7]. In this work, we use EF gasifiers as they are more suitable for large scale processes and have the advantage of complete tar cracking and removal [15, 16].

Tire-derived syngas typically has a $H_2$/CO molar ratio of $\sim$ 0.4 - 1.1 [7].

In our previous work, we implemented the option to use a water gas shift (WGS) process to upgrade the syngas prior to downstream synthesis. A more efficient alternative may be to include natural gas as an additional feedstock to produce hydrogen-rich syngas that can be blended with tire-derived syngas. Two configurations are presented by Adams and Barton for combining EF gasification and natural gas reforming: Internal reforming and external reforming [3]. Internal reforming involves filling the tubes of the radiant syngas cooler (RSC) of the EF gasifier with natural gas, water and reforming catalyst such that the absorbed heat is used to drive the endothermic natural gas conversion process. A further development proposed by Hoseinzade and Adams involves implementing dry reforming in the RSC tubes by using $CO_2$ instead of steam as a reforming agent [17]. External reforming involves implementing an auto-thermal reformer (ATR) outside the gasifier in which pre-reformed natural gas is mixed with steam and oxygen from an Air Separation Unit (ASU). While internal reforming has been shown to give better economic and thermodynamic performance [3, 9], this configuration involves additional complexity and has limited flexibility in that the flow rates of natural gas and waste tire need to be matched (within relatively narrow constraints) for appropriate heat integration to occur. Conversely, in external reforming, the ATR and EF gasifier are completely decoupled allowing a wide range of throughputs, thus this option is implemented in this work. Allowing for a variation in feedstock flow rates is particularly relevant if flexible polygeneration is to be implemented such that the optimal product portfolio is adjusted in order to respond to market conditions (as detailed in our follow-up work [18] and [19]). Another alternative for methane conversion is dry reforming using a $CO_2$ feed stream. While this allows $CO_2$ utilization, it may require a large amount of steam at the later water-gas shift stage in order to achieve the appropriate $H_2/CO$ ratio. Thus, in this work, we choose the extensively used steam methane reforming that generates syngas with a higher $H_2/CO$ ratio. We note that the objective of minimizing $CO_2$ emissions is accounted for by imposing a $CO_2$ tax as part of the annual operating expenses.

Several other research efforts have investigated the use of a hybrid of a conventional and alternative feedstock. Meerman et al. studied the conversion of coal, biomass and oil residues to hydrogen, Fischer-Tropsch liquids, methanol, urea and electricity [20, 21]. The economic value of implementing various levels of flexibility was determined and an analysis on the favorability of each feedstock and product for a given price scenario was presented. Okeke

and Adams studied different configurations for converting a hybrid petcoke and natural gas feedstock to Fischer-Tropsch (FT) liquids, with the results highlighting the value of implementing the internal reforming strategy [9]. However, in all these works, optimization of the system design and operating conditions was not carried out. Martin and Grossmann study the use of a hybrid switchgrass and shale gas feedstock to produce hydrogen and liquid fuels using a superstructure optimization approach [22]. They investigate the feedstock prices at which the switchgrass and shale feedstocks are favored. Santibanez-Aguilar et al. developed a supply chain optimization model for the conversion and distribution of biomass [23]. Several products are considered for the biorefinery and a multiple objectives are studied with a conclusion that paying attention to particular geographical attributes is highly relevant to determining the optimal supply chain. Chen et al. presented the globally optimal design of a process that converts coal and biomass to naphtha, diesel, methanol and electricity, and concluded that the carbon tax rate and biomass price substantially influenced the degree to which biomass is utilized [11, 24]. Both feedstocks were converted in a single gasification unit, thus the option of generating multiple syngas streams followed by subsequent blending was not studied. Baliban et al. investigated a process for conversion of biomass, coal and natural gas to liquid fuels and studied the impact of implementing $CO_2$ capture on the break-even prices [25]. Salkuyeh and Adams investigated the optimal design of a petcoke and natural gas feedstock polygeneration process that produces methanol, dimethyl ether (DME), olefins and electricity [10].

Although the studies above highlight the value in using a hybrid of a conventional and alternative feedstock in general, further research is necessary to analyze the co-utilization of waste tires and natural gas. Furthermore, the authors seek to address a gap in the literature by systematically investigating the synergies that can be obtained by using a mix of waste tires (converted using an EF gasifier) and natural gas (converted using an ATR). This work also carries out rigorous process modeling and simulation as well as techno-economic optimization. Thus, the objective of this paper is to study the globally optimal design and operation of a hybrid waste tire and natural gas feedstock polygeneration system under a variety of economic and policy conditions. This work also provides a detailed description of the process and the optimization model which is relevant to our follow up work on the design of flexible polygeneration systems using a stochastic programming approach [18, 19].

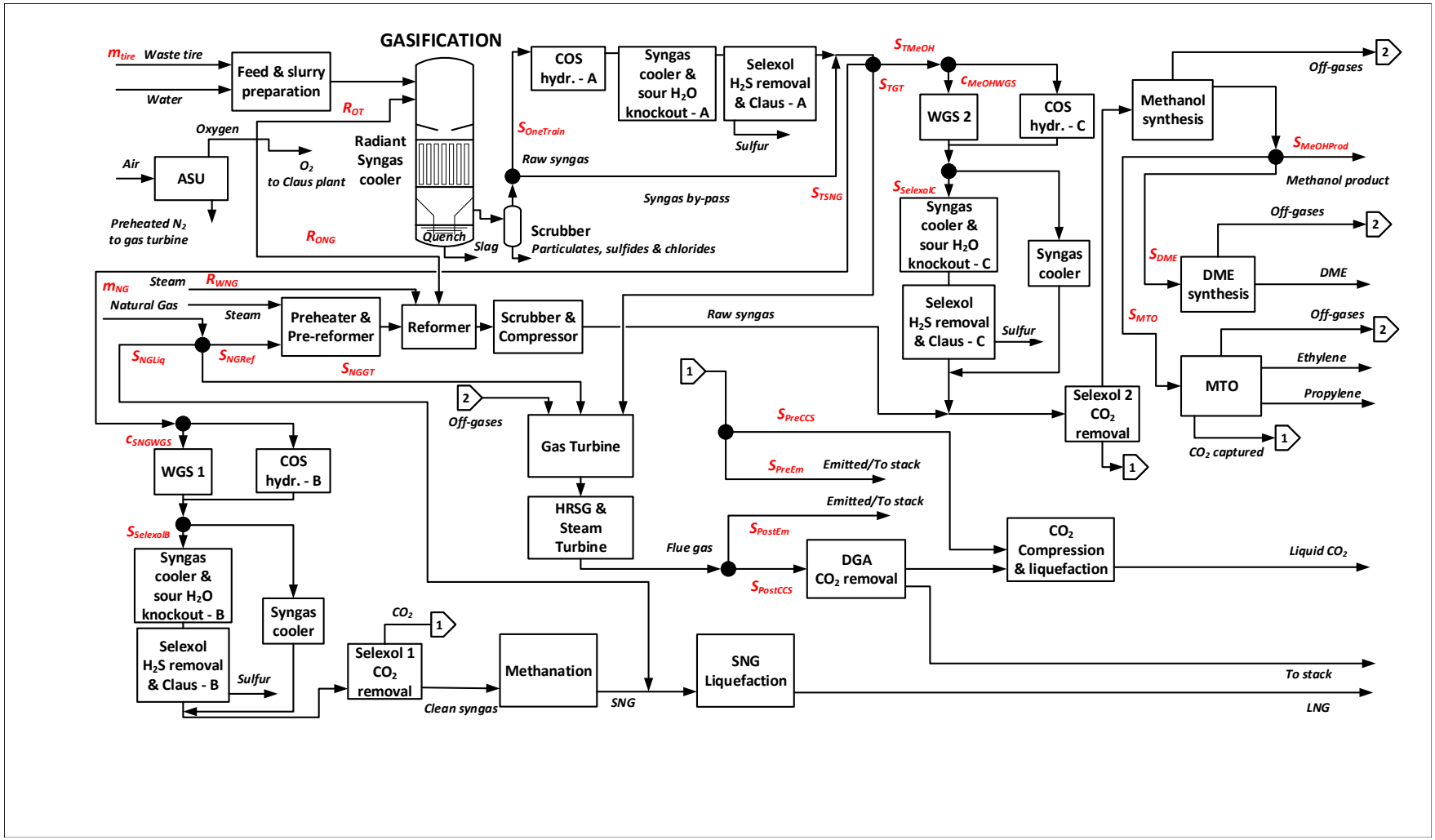


Figure 1: Superstructure of the hybrid natural gas and waste tire feedstock polygeneration system. The operational decision variables are indicated in red and presented in Figure 2

## 2. Process Simulation, Surrogate Modeling and Optimization Problem formulation

Figure 1 presents a superstructure of the hybrid waste tire and natural gas feedstock polygeneration system for the production of electricity, methanol, DME, olefins or LNG. Two kinds of decision variables are considered: Design decision variables (denoted $\mathbf{y}$) and operational decision variables (denoted $\mathbf{x}$). Design decision variables are used to determine the sizing of the various process sections as discussed in Section 2.4. Operational decision variables are indicated in red in Figure 1 and presented in Figure 2. The mass flow rate of tire ($m_{tire}$) and natural gas ($m_{NG}$) are the only extensive operational decision variables. The total thermal input is constrained to be less than 893 MW so as to provide fair comparison with previous work [15, 6]. Similar to our previous work [7], we use the following three-step procedure to formulate the optimization problem:

- First, we implement rigorous process models for the mass and energy balance calculations using either Aspen HYSYS v10 (for the Selexol units) or Aspen Plus v10 (for all other sections). The operating conditions and specifications used in the simulation are detailed in the Supplementary Material. The thermodynamic property packages used are also detailed in [7].

- Next, we sample these rigorous process models to generate data that are used to fit surrogate mass and energy balance models for the various process sections. The ALAMO software package was used for fitting surrogate algebraic models for each section [26, 27]. The details of the basis functions and coefficients used are presented in the Supplementary Material.

- Finally, we formulate these algebraic surrogate models as equality constraints of the optimization problem. In addition, we include the economic models for the capital cost and annual net profit calculations as discussed in Section 2.4. Net Present Value (NPV) is calculated and used as the objective function. In this work, we use the (C++-based) modeling language native to the recently developed GOSSIP software framework [28]. GOSSIP contains subroutines for parsing the user-defined model, pre-processing and linking to state-of-the-art global optimization solvers such as ANTIGONE [29]. GOSSIP also includes

a utility to generate a GAMS model which was used in this work. We note that GOSSIP also includes implementations of novel decomposition algorithms for solving two-stage stochastic programs (such as Nonconvex Generalized Benders Decomposition [30], [31] and Lagrangian relaxation-based approaches [28]). However, these are not used in this work but are relevant to our follow up work [18, 19].

The complete optimization model is presented in the Supplementary Material. In the following sections, an overview of the most important process sections is presented.

*2.1. Natural gas train*

The natural gas stream is split into three branches that lead to the liquefaction section to produce LNG, the gas turbine section to produce electricity, or a downstream methanol synthesis train, with $S_{NGLiq}$, $S_{NGGT}$, $S_{NGRef}$ denoting the corresponding split fractions. The natural gas stream heading to the methanol train is first pre-heated and pre-reformed by adding steam to convert most of the higher hydrocarbons to syngas. The pre-reformed stream then heads to an ATR and is mixed with steam and oxygen in ratios given by the $R_{WNG}$ and $R_{ONG}$ decision variables respectively. The ATR is modeled using an RGIBBS reactor assuming restricted chemical equlibrium as detailed in [9]. Four reactions (Equations NG1, NG2, NG3, NG4) occur in the ATR:

$$\mathrm{CO} + 3\,\mathrm{H_2} \rightleftharpoons \mathrm{CH_4} + \mathrm{H_2O} \tag{NG1}$$

$$\mathrm{CO} + \mathrm{H_2O} \rightleftharpoons \mathrm{H_2} + \mathrm{CO_2} \tag{NG2}$$

$$\mathrm{CH_4} + 2\,\mathrm{O_2} \rightleftharpoons \mathrm{CO_2} + 2\,\mathrm{H_2O} \tag{NG3}$$

$$2\,\mathrm{CO} + \mathrm{O_2} \rightleftharpoons 2\,\mathrm{CO_2} \tag{NG4}$$

The surrogate model for the extent of each reaction $r$ ($\xi_{r,NGRef}$) is presented in Equation 1 highlighting the dependence on the relevant decision

variables $m_{NGRef}$, $R_{ONG}$ and $R_{WNG}$, with the values of the coefficients presented in the Supplementary Material.

$$\begin{aligned}\xi_{r,NGRef} = m_{NGRef}\cdot(&\beta_{0,NGRef,r}+\beta_{1,NGRef,r}\cdot R_{ONG}+\beta_{2,NGRef,r}\cdot R_{ONG}^2+\beta_{3,NGRef,r}\cdot R_{ONG}^3\\ &+\beta_{4,NGRef,r}\cdot R_{ONG}^4+\beta_{5,NGRef,r}\cdot exp(R_{ONG})+\beta_{6,NGRef,r}\cdot log(R_{ONG})\\ &+\alpha_{0,NGRef,r}+\alpha_{1,NGRef,r}\cdot R_{WNG}+\alpha_{2,NGRef,r}\cdot R_{WNG}^2+\alpha_{3,NGRef,r}\cdot R_{WNG}^3\\ &+\alpha_{4,NGRef,r}\cdot R_{WNG}^4+\alpha_{5,NGRef,r}\cdot exp(R_{WNG})+\alpha_{6,NGRef,r}\cdot log(R_{WNG}))\\ &\forall r \in \{\text{NG1, NG2, NG3, NG4}\}\end{aligned} \tag{1}$$

Species mass balance in the ATR is enforced by an additional constraint (Equation 2), where $f_{NGRef\_in,i}$ and $f_{NGRef\_prod,i}$ denote the molar flow rates of component $i$ in the stream entering and leaving the ATR respectively, and $\nu_{i,r}$ denotes the stoichiometric coefficient of component $i$ in reaction $r$.

$$f_{NGRef\_prod,i} = f_{NGRef\_in,i} + \sum_r \nu_{i,r}\cdot\xi_{r,NGRef},\ \forall i \in I, \tag{2}$$

A similar strategy is used to generate the energy balance model. The reformed syngas is then cooled, dried and compressed prior to downstream synthesis.

### *2.2. Waste tire train*

Waste tires received at the plant gates are ground and processed into crumbs and then mixed with water. The tire slurry combined with oxygen from the ASU is sent to an EF gasifier that generates syngas that is then cooled in the RSC, quenched and scrubbed to remove particulates, sulfides and chlorides [32]. The solid impurities flow down the walls of the gasifier, through the throat and exit as slag [3]. The gasifier operating temperature and the syngas composition is determined by the ratio of the oxygen to waste tire mass flow rate ($R_{OT}$).

Details of the simulation strategy of the gasifier are presented in [7] and [33]. In brief: Tire decomposition to reactive species is modeled using an RYIELD block (together with a calculator block to enforce atomic balance between the species and the tire feedstock as quantified by ultimate composition). An RGIBBS block assuming chemical equilibrium is then used to

convert the reactive species to syngas. A similar approach to generating surrogate mass and energy balance models as the natural gas reforming section is used as detailed in the Supplementary Material.

Considering that tire-generated syngas contains a non-negligible amount of sulfur-containing compounds (COS and $H_2S$), gas cleaning is essential. Sulfur removal consists of a series of three steps: First, a COS hydrolysis reaction is implemented to convert any COS to $H_2S$, next the syngas is cooled and sour water is knocked out and treated, finally a Selexol-based $H_2S$ removal system coupled with a Claus process is implemented. Either the entire raw syngas stream from the gasifier can be diverted to a "One Train" sulfur removal section ($S_{OneTrain}$ denotes this binary choice) or the sulfur removal can be implemented after a stream split to the methanation or methanol synthesis sections. The advantage of the latter option is that if WGS is implemented prior to product synthesis, COS hydrolysis takes place simultaneously thus eliminating the need for a dedicated reactor.

### *2.3. Downstream synthesis & Power generation sections*

Tire-derived syngas is split into three branches heading to the methanation, methanol synthesis and power generation sections according to the $S_{TSNG}$, $S_{TMeOH}$ and $S_{TGT}$ split fractions respectively. In both methanation and methanol synthesis sections, the $H_2$/CO ratio of the tire-derived syngas can be adjusted by implementing WGS reactors with the corresponding conversions given by $c_{SNGWGS}$ and $c_{MeOHWGS}$ respectively. If WGS is not implemented, then the stream passes through a separate COS hydrolysis reactor, followed by a sulfur removal system. For the methanol synthesis section, the $H_2$/CO ratio can also be adjusted by blending with the hydrogen-rich natural gas-derived syngas stream. $CO_2$ is then removed from syngas in either of the synthesis trains using a Selexol-based process. Purified methanol can be sold as final product or diverted to the DME or MTO sections according to the $S_{MeOHProd}$, $S_{DME}$, or $S_{MTO}$ split fractions. Only linear surrogate mass and energy balance models are used for both synthesis sections since all intensive operating conditions are held constant with details available in our previous work [7] and the Supplementary Material.

After power generation in the gas turbine, additional electricity is generated using a Heat Recovery Steam Generator (HRSG) and steam turbine system. Energy balance constraints are implemented by assuming constant turbine efficiency such that the net work generated is a linear function of the thermal inputs (on a LHV basis) of the streams heading to the corresponding

sections. The quantity of work generated in the steam turbine is determined using the approach presented in Chen et al. [11] where the background heat is divided into high and low quality heat each converted using at an efficiency value detailed in the Supplementary Material.

Flue gases either head to the DGA-based postcombustion $CO_2$ capture system (with split fraction denoted by $S_{PostCCS}$) or are emitted (split fraction $S_{PostEm}$). Similarly $CO_2$ captured in the methanation, methanol synthesis or MTO trains is either compressed, liquefied and sent for sequestration (with split fraction given by $S_{PreCCS}$) or emitted (split fraction $S_{PreEm}$).

### *2.4. Economic modeling & Optimization problem formulation*

The optimal design and operation problem (with decision variables $\mathbf{y}$ and $\mathbf{x}$) is solved for two case studies: Without and with waste tire tipping fees of 100 \$/tonne. For each case study, 6 scenarios for the product prices and $CO_2$ tax rates are considered as presented in Figure 3. Based on these parameters and the process model, the annual revenues are determined. Fixed annual operating costs (labor, maintenance, operating overhead, and property insurance & tax costs) are estimated based on the approach of Seider et al. [34] while variable operating costs (electricity, utilities, feedstock, solvent & catalyst and waste disposal costs) are determined based on the process model together with price parameters estimated from literature sources [32]. Following this, the annual operating profit ($Pro_{net}$) is calculated.

Capital costs ($Cap$) are determined based on the binary design decision variables $\mathbf{y}$. Each process section can take on one size from a discrete set of equipment sizes (as detailed in [7, 24]); the corresponding capital cost is determined using a scaling relation based on reference data as detailed in the Supplementary Material. The NPV is used as the objective function (Equation 3) calculated using the Discounted Cash Flow Rate of Return approach similar to [24].

The nonconvex MINLP optimization problem is solved to global optimality using ANTIGONE [29]. Nonconvexities generally result from bilinear terms in the mass and energy balance models. In addition, the fitted surrogate models for the gasifier and natural gas reformer are highly nonlinear equality constraints. In summary, the optimization problem has the following variables and constraints:

- 280 binary design variables (used to represent the choice of one of 10 sizes for each of the 28 process sections)

- 1054 continuous operational variables
- 5 binary operational variables
- 28 inequality constraints involving the binary design variables
- 1054 constraints involving the continuous variables.

In brief, the global optimization solver solves a series of lower bounding and upper bounding optimization problems that bracket the global optimum. The lower bounding problems provide a lower estimate on the global optimum and are generally solved by formulating a convex relaxation of the original problem. The upper bounding problem provides an upper estimate of the global optima which is commonly provided by a local optimum of the nonconvex problem. The domain of the variables is then successively made smaller until convergence within a given tolerance. Multiple optimization jobs are run in parallel using the grid computing option within GAMS on an AMD EPYC 64 core (and 2.60 GHz) computer with 512 GB of RAM. A relative gap (UBD-LBD/UBD) of 0.001 is used as a termination criterion for global optimality.

| Decision Variable | Description | Units | LBD | UBD |
|---|---|---|---|---|
| Waste tire train | | | | |
| $m_{tire}$ | Mass flow rate of waste tire feedstock | kg/s | 0.0 | 26.3 |
| $R_{OT}$ | Ratio of (pure) oxygen to waste tire sent to gasifier (mass basis) | | 0.25 | 1.25 |
| $S_{OneTrain}$ | Binary variable for choice of one train sulfur removal system vs. by-pass | | 0 | 1 |
| $S_{TSNG}$ | Split fraction of tire-derived syngas sent to methanation | | 0.0 | 1.0 |
| $S_{TMeOH}$ | Split fraction of tire-derived syngas sent to methanol synthesis | | 0.0 | 1.0 |
| $S_{TGT}$ | Split fraction of tire-derived syngas sent to the gas turbine | | 0.0 | 1.0 |
| Natural gas train | | | | |
| $m_{NG}$ | Mass flow rate of natural gas feedstock | kg/s | 0.0 | 18.7 |
| $S_{NGRef}$ | Split fraction of natural gas sent to reformer | | 0.0 | 1.0 |
| $S_{NGGT}$ | Split fraction of the natural gas sent to gas turbine | | 0.0 | 1.0 |
| $S_{NGLiq}$ | Split fraction of the natural gas sent for liquefaction | | 0.0 | 1.0 |
| $R_{ONG}$ | Ratio of (pure) oxygen to natural gas fed to reformer (mass basis) | | 0.95 | 1.12 |
| $R_{WNG}$ | Ratio of steam to natural gas fed to reformer (mass basis) | | 0.75 | 1.5 |
| Downstream product trains | | | | |
| $c_{SNGWGS}$ | Conversion of CO in the WGS reactor in the methanation train | | 0.0 | 0.8 |
| $c_{MeOHWGS}$ | Conversion of CO in the WGS reactor in the methanol synthesis train | | 0.0 | 0.8 |
| $S_{SelexolB}$ | Binary variable for choice of sulfur removal prior to methanation vs. by-pass | | 0 | 1 |
| $S_{SelexolC}$ | Binary variable for choice of sulfur removal prior to methanol synthesis vs. by-pass | | 0 | 1 |
| $S_{MeOHProd}$ | Split fraction of methanol product | | 0.0 | 1.0 |
| $S_{DME}$ | Split fraction of methanol diverted for synthesis of DME | | 0.0 | 1.0 |
| $S_{MTO}$ | Split fraction of methanol diverted for synthesisof olefins | | 0.0 | 1.0 |
| $CO_2$ capture train | | | | |
| $S_{PostCCS}$ | Split fraction of flue gas sent to the DGA process for postcombustion $CO_2$ capture | | 0.0 | 1.0 |
| $S_{PreCCS}$ | Split fraction of captured $CO_2$ from the rest of the plant sent for sequestration | | 0.0 | 1.0 |
| $S_{PostEm}$ | Split fraction of flue gas sent to stack/emitted | | 0.0 | 1.0 |
| $S_{PreEm}$ | Split fraction of emitted $CO_2$ removed from the rest of the plant | | 0.0 | 1.0 |

Figure 2: List of the 23 operational decision variables for the optimization problem and their bounds

| Parameter | Description | Units | S1 Historical | S2 $\uparrow P_{NG}$ | S3 $\uparrow P_{MeOH}$ | S4 $\uparrow P_{DME}$ | S5 $\uparrow P_{Olefins}$ [2] | S6 $\uparrow P_{CO_2}$ | $\sigma$ |
|---|---|---|---|---|---|---|---|---|---|
| $P_{NG}$ [1] | Natural gas prices | \$/MMBtu | 5.5 | 14.4 | 5.5 | 5.5 | 2.1 | 5.5 | 3.0 |
| $P_{Elec}$ | Hourly elec. price | \$/MWh | 96.1 | 96.1 | 96.1 | 96.1 | 50.0 | 96.1 | 22.1 |
| $P_{MeOH}$ | Methanol price | \$/tonne | 500 | 500 | 700 | 500 | 100 | 500 | 200 |
| $P_{DME}$ | DME price | \$/tonne | 800 | 800 | 800 | 1000 | 200 | 800 | 200 |
| $P_{Ethylene}$ | Ethylene price | \$/tonne | 1050 | 1050 | 1050 | 1050 | 3400 | 1050 | 360 |
| $P_{Propylene}$ | Propylene price | \$/tonne | 1000 | 1000 | 1000 | 1000 | 3600 | 1000 | 400 |
| $P_{CO_2}$ | $CO_2$ tax rate | \$/tonne | 0 | 0 | 0 | 0 | 0 | 100 | 25 |

Figure 3: Prices and $CO_2$ tax rate parameters for the scenarios S1 - S6 considered for each of the 2 case studies (without and with waste tire tipping fees). $\sigma$ denotes standard deviation based on historical data assuming normal distributions. [1] A fixed premium of 65% is assumed for the price of LNG over the price of natural gas based on data from [35]. [2] $P_{Olefins}$ denotes the price of ethylene and propylene.

$$
\begin{aligned}
\max_{\mathbf{y},\,\mathbf{x}} \quad & \text{Net Present Value} \\
\text{s.t.} \quad & \text{Surrogate Mass and energy balances model} \\
& \text{Scale Constraint} \\
& \text{Operating cost model} \\
& \text{Capital cost model} \\
& \text{Annual Net Profit model}
\end{aligned}
\tag{3}
$$

## 3. Results and Discussion

Figure 4 presents the optimal values of the operational decision variables for Case 1. Figure 5 presents the corresponding capital costs, product portfolio, as well as the thermodynamic, environmental and economic performance. Figures 6 and 7 present analogous results for Case 2. In the product portfolio section, the values in brackets denote the fraction of the relevant product by energy content.

### *3.1. Case 1: Without waste tire tipping fees*

In scenario S1 (historically average product prices), natural gas is used as a single feed stream and electricity is generated as the only product. Thus, synergies between the multiple feedstock or product trains are not exploited and polygeneration does not occur under these market conditions. Similarly in scenario S2 ($P_{NG}$ $3\sigma$ above average), only natural gas is used and only a liquefaction process is implemented to produce LNG. Thus, the discounted capital and operating costs of liquefaction are exceeded by the price premium of LNG over natural gas.

However, in scenarios S3 ($P_{MeOH}$ $1\sigma$ above average), S4 ($P_{DME}$ $1\sigma$ above average) and S5 ($P_{Ethylene}$ and $P_{Propylene}$ $6\sigma$ above average and other prices below average) where methanol, DME and olefins are favored as the primary product respectively, both waste tire and natural gas are used thus synergies between the two feedstock trains are exploited. For instance, in these three cases, waste tire gasification produces hydrogen-lean syngas ($H_2$/CO ratio of $\sim 0.7$) which is mixed with hydrogen-rich syngas ($H_2$/CO ratio of $\sim 3.0$) from natural gas reforming to get the correct ratio of $\sim 2.0$ for methanol synthesis. We note that two configurations of the relevant decision variables

result in generating the right quality of syngas: The first configuration (used in scenario S3 and S5) involves using a lower $m_{tire}$ of $\sim$ 8.2-8.3 kg/s and a higher $m_{NG}$ of 12.8-12.9 kg/s, while the second configuration (used in S4) involves using a higher $m_{tire}$ of $\sim$ 12.4 kg/s together with syngas upgrading using WGS, and a lower $m_{NG}$ of 9.8 kg/s. The trade-offs involved are as follows: Natural gas is a more expensive feedstock but generally results in a higher yield of hydrogen-rich syngas which does not require sulfur removal while waste tire is a zero cost feedstock whose gasification generates high quality heat but requires expensive sulfur removal and generates lower yields of hydrogen-lean syngas. The results imply that both of these configurations correspond to different global optima with objective function values lying within the relative tolerance used. Lastly, we note that scenario S5 has a low probability of occurring thus the production of olefins is rarely favored.

In scenario S6, carbon taxes are imposed which result in a switch in primary product from electricity to methanol. This can be explained by the fact that a substantial portion of $CO_2$ is emitted in flue gas after the gas turbine for electricity generation. However, in the methanol train, a smaller quantity of $CO_2$ is removed prior to synthesis as a greater proportion of carbon atoms from the feedstock are kept in the MeOH product.

### *3.2. Case 2: With waste tire tipping fees of 100 $/tonne*

Larger quantities of waste tire are used in all market scenarios in Case 2. However, in general this results in a lower energy efficiency.

In scenario S1, methanol is favored instead as the major product primarily from upgraded tire-derived syngas. However, a small amount of natural gas is used with the feedstock stream split between the methanol and electricity trains. Thus, polygeneration occurs in this scenario. However, we note that the reason multiple products were favored is because of the imposition of certain constraints (namely a constraint on the total thermal input to the plant, a constraint that all pieces of equipment can only take on discrete sizes, and a constraint on correct syngas ratios for product synthesis). We also note that in S1 (for both Cases), the decision to produce methanol versus electricity is highly sensitive to prevailing market conditions resulting in a difficult optimization problem that takes longer for convergence to the global optimum. This motivates our follow-up work on the design of a flexible polygeneration process (using a stochastic programming approach) that is able to adjust operating conditions to exploit market conditions by producing a changing product portfolio ([19] extended in [18]). Furthermore, we expect

the one train sulfur system to be more relevant for such a flexible design as implementing separate gas cleaning systems for each product train would be expensive.

Scenarios S2 to S5 result in designs that favor the product that experiences a higher price while $CO_2$ capture and liquefaction (for sequestration) is implemented in S6. Similar to Case 1, multiple optimal (within the tolerance considered) configurations of the decision variables result in generating the correct quality of syngas. Finally, we note that for cases in which a literature comparison is available, the thermodynamic performance of the proposed processes reported in Tables 5 and 7 are in a similar range. For instance, the energy efficiency values for scenario S1 of Case 1 are in line with the range reported by Jordal et al. [36] for the production of electricity from natural gas. Efficiency values for cases S2 - S6 for the production of methanol, DME and olefins are in a similar range to those reported by Salkuyeh et al. [37].

| **Case** | Units | S1 | S2 | S3 | S4 | S5 | S6 |
|---|---|---|---|---|---|---|---|
| | | Historical | $\uparrow P_{NG}$ | $\uparrow P_{MeOH}$ | $\uparrow P_{DME}$ | $\uparrow P_{Olefins}$ [1] | $\uparrow P_{CO_2}$ |
| Waste tire train | | | | | | | |
| $m_{tire}$ | kg/s | 0.0 | 0.0 | 8.3 | 12.4 | 8.2 | 8.7 |
| $R_{OT}$ | | 0.000 | 0.000 | 0.887 | 0.887 | 0.887 | 0.887 |
| $S_{OneTrain}$ | | 0 | 0 | 0 | 0 | 0 | 0 |
| $S_{TSNG}$ | | 0.0 | 0.0 | 0.0 | 0.0 | 0.0 | 0.0 |
| $S_{TMeOH}$ | | 0.0 | 0.0 | 1.0 | 1.0 | 1.0 | 1.0 |
| $S_{TGT}$ | | 0.0 | 0.0 | 0.0 | 0.0 | 0.0 | 0.0 |
| Natural gas train | | | | | | | |
| $m_{NG}$ | kg/s | 18.7 | 18.7 | 12.8 | 9.8 | 12.9 | 12.5 |
| $S_{NGRef}$ | | 0.0 | 0.0 | 1.0 | 1.0 | 1.0 | 1.0 |
| $S_{NGGT}$ | | 1.0 | 0.0 | 0.0 | 0.0 | 0.0 | 0.0 |
| $S_{NGLiq}$ | | 0.0 | 1.0 | 0.0 | 0.0 | 0.0 | 0.0 |
| $R_{ONG}$ | | 0.000 | 0.000 | 0.950 | 0.950 | 0.958 | 0.950 |
| $R_{WNG}$ | | 0.000 | 0.000 | 0.750 | 1.500 | 0.750 | 0.855 |
| Downstream product trains | | | | | | | |
| $c_{SNGWGS}$ | | 0.000 | 0.000 | 0.000 | 0.000 | 0.000 | 0.000 |
| $c_{MeOHWGS}$ | | 0.000 | 0.000 | 0.000 | 0.100 | 0.000 | 0.425 |
| $S_{SelexolB}$ | | 0 | 0 | 0 | 0 | 0 | 0 |
| $S_{SelexolC}$ | | 0 | 0 | 1 | 1 | 1 | 1 |
| $S_{MeOHProd}$ | | 0.0 | 0.0 | 1.0 | 0.0 | 0.0 | 1.0 |
| $S_{DME}$ | | 0.0 | 0.0 | 0.0 | 1.0 | 0.0 | 0.0 |
| $S_{MTO}$ | | 0.0 | 0.0 | 0.0 | 0.0 | 1.0 | 0.0 |
| $CO_2$ capture train | | | | | | | |
| $S_{PostCCS}$ | | 0.0 | 0.0 | 0.0 | 0.0 | 0.0 | 1.0 |
| $S_{PreCCS}$ | | 0.0 | 0.0 | 0.0 | 0.0 | 0.0 | 1.0 |
| $S_{PostEm}$ | | 1.0 | 1.0 | 1.0 | 1.0 | 1.0 | 0.0 |
| $S_{PreEm}$ | | 1.0 | 1.0 | 1.0 | 1.0 | 1.0 | 0.0 |

Figure 4: Optimal values of the operational decision variables for Case 1 (Without Waste Tire tipping fees). The corresponding economic results are in Figure 5. [1] $P_{Olefins}$ denotes the price of ethylene and propylene.

| **Case** | | S1 | S2 | S3 | S4 | S5 | S6 |
|---|---|---|---|---|---|---|---|
| **Capital costs** | | | | | | | |
| Waste tire train | | | | | | | |
| Gasifier | M$ | 0.0 | 0.0 | 135.3 | 176.5 | 129.5 | 135.3 |
| One train sulfur removal | M$ | 0.0 | 0.0 | 0.0 | 0.0 | 0.0 | 0.0 |
| Natural gas train | | | | | | | |
| Reformer | M$ | 0.0 | 0.0 | 48.0 | 42.0 | 48.0 | 48.0 |
| Liquified (Synthetic) NG train | | | | | | | |
| WGS 1 | M$ | 0.0 | 0.0 | 0.0 | 0.0 | 0.0 | 0.0 |
| Sulfur removal | M$ | 0.0 | 0.0 | 0.0 | 0.0 | 0.0 | 2.7 |
| $CO_2$ removal | M$ | 0.0 | 0.0 | 0.0 | 0.0 | 0.0 | 13.7 |
| Methanation | M$ | 0.0 | 0.0 | 0.0 | 0.0 | 0.0 | 28.6 |
| Liquefaction | M$ | 0.0 | 31.8 | 0.0 | 0.0 | 0.0 | 10.8 |
| Methanol train | M$ | 0.0 | 0.0 | 0.0 | 9.7 | 0.0 | 0.0 |
| WGS 2 | M$ | 0.0 | 0.0 | 0.0 | 9.7 | 0.0 | 0.0 |
| Sulfur removal | M$ | 0.0 | 0.0 | 33.1 | 27.9 | 35.7 | 33.1 |
| $CO_2$ removal | M$ | 0.0 | 0.0 | 19.6 | 19.6 | 19.6 | 19.6 |
| Methanol synthesis | M$ | 0.0 | 0.0 | 81.2 | 81.2 | 81.2 | 81.2 |
| DME synthesis | M$ | 0.0 | 0.0 | 0.0 | 92.1 | 0.0 | 0.0 |
| MTO | M$ | 0.0 | 0.0 | 0.0 | 0.0 | 224.1 | 0.0 |
| Power system | M$ | 353.3 | 0.0 | 110.2 | 110.2 | 160.3 | 110.2 |
| DGA | M$ | 0.0 | 0.0 | 0.0 | 0.0 | 0.0 | 31.3 |
| $CO_2$ compression & sequestration | M$ | 0.0 | 0.0 | 0.0 | 0.0 | 0.0 | 4.6 |
| ASU | M$ | 0.0 | 0.0 | 164.6 | 164.6 | 164.6 | 164.6 |
| Water systems | M$ | 0.0 | 0.0 | 63.2 | 63.2 | 63.2 | 63.2 |
| Miscellaneous | M$ | 52.6 | 52.6 | 52.6 | 52.6 | 52.6 | 52.6 |
| Total capital costs ($Cap$) | M$ | 405.9 | 84.4 | 707.9 | 839.7 | 979.0 | 799.5 |
| **Product portfolio** | | | | | | | |
| Liquefied SNG | kg/s | 0.0 | 18.7 (100.0%) | 0.0 | 0.0 | 0.0 | 0.0 |
| Electricity | MW | 544.2 (100.0%) | -18.7 | 14.4 (2.3%) | 14.6 (2.8%) | 48.6 (21.7%) | 8.0 (1.3%) |
| Methanol | kg/s | 0.0 | 0.0 | 28.5 (97.7%) | 0.0 | 0.0 | 28.3 (98.7%) |
| DME | kg/s | 0.0 | 0.0 | 0.0 | 16.7 (97.2%) | 0.0 | 0.0 |
| Ethylene | kg/s | 0.0 | 0.0 | 0.0 | 0.0 | 2.0 (42.0%) | 0.0 |
| Propylene | kg/s | 0.0 | 0.0 | 0.0 | 0.0 | 1.8 (36.3%) | 0.0 |
| **Thermodynamic performance** | | | | | | | |
| Total thermal output | MW | 544.2 | 874.3 | 615.7 | 514.5 | 223.8 | 606.6 |
| Thermal efficiency (LHV) | % | 60.9 | 97.9 | 68.9 | 57.6 | 25.1 | 67.9 |
| **Environmental performance** | | | | | | | |
| Direct $CO_2$ emissions | kg/s | 50.0 | 0.0 | 16.7 | 21.7 | 25.8 | 0.3 |
| $CO_2$ sequestered | kg/s | 0.0 | 0.0 | 0.0 | 0.0 | 0.0 | 16.9 |
| **Economic performance** | | | | | | | |
| Annual Net Profit ($Pro_{net}$) | M$/year | 128.0 | 97.6 | 244.9 | 205.1 | 173.9 | 147.3 |
| Net Present Value (NPV) | M$ | 594.4 | 653.4 | 1198.4 | 784.0 | 427.2 | 388.1 |
| Total wall time (ANTIGONE) | s | 8302 | 4279 | 3511 | 4234 | 1391 | 5687 |

Figure 5: Capital costs, Product portfolio, Thermodynamic, Environmental and Economic performance of the proposed concept for Case 1 (Without Waste Tire tipping fees) under the 6 scenarios studied.

| **Case** | Units | S1 | S2 | S3 | S4 | S5 | S6 |
|---|---|---|---|---|---|---|---|
| | | Historical | $\uparrow P_{NG}$ | $\uparrow P_{MeOH}$ | $\uparrow P_{DME}$ | $\uparrow P_{Olefins}$ [1] | $\uparrow P_{CO_2}$ |
| Waste tire train | | | | | | | |
| $m_{tire}$ | kg/s | 23.3 | 25.3 | 17.4 | 26.3 | 17.4 | 25.3 |
| $R_{OT}$ | | 0.887 | 0.869 | 0.887 | 0.836 | 0.887 | 0.869 |
| $S_{OneTrain}$ | | 0 | 0 | 0 | 0 | 0 | 0 |
| $S_{TSNG}$ | | 0.0 | 1.0 | 0.0 | 0.0 | 0.0 | 0.0 |
| $S_{TMeOH}$ | | 1.0 | 0.0 | 1.0 | 1.0 | 1.0 | 1.0 |
| $S_{TGT}$ | | 0.0 | 0.0 | 0.0 | 0.0 | 0.0 | 0.0 |
| Natural gas train | | | | | | | |
| $m_{NG}$ | kg/s | 2.1 | 0.7 | 6.3 | 0.0 | 6.3 | 0.7 |
| $S_{NGRef}$ | | 0.5 | 0.0 | 1.0 | 0.0 | 1.0 | 0.0 |
| $S_{NGGT}$ | | 0.5 | 0.0 | 0.0 | 0.0 | 0.0 | 1.0 |
| $S_{NGLiq}$ | | 0.0 | 1.0 | 0.0 | 0.0 | 0.0 | 0.0 |
| $R_{ONG}$ | | 1.0 | 0.0 | 1.0 | 0.0 | 1.0 | 0.0 |
| $R_{WNG}$ | | 1.5 | 0.0 | 1.5 | 0.0 | 0.9 | 0.0 |
| Downstream product trains | | | | | | | |
| $c_{SNGWGS}$ | | 0.000 | 0.571 | 0.000 | 0.000 | 0.000 | 0.000 |
| $c_{MeOHWGS}$ | | 0.416 | 0.000 | 0.282 | 0.408 | 0.322 | 0.426 |
| $S_{SelexolB}$ | | 0 | 1 | 0 | 0 | 0 | 0 |
| $S_{SelexolC}$ | | 1 | 0 | 1 | 1 | 1 | 1 |
| $S_{MeOHProd}$ | | 1.0 | 0.0 | 1.0 | 0.0 | 0.0 | 1.0 |
| $S_{DME}$ | | 0.0 | 0.0 | 0.0 | 1.0 | 0.0 | 0.0 |
| $S_{MTO}$ | | 0.0 | 0.0 | 0.0 | 0.0 | 1.0 | 0.0 |
| $CO_2$ capture train | | | | | | | |
| $S_{PostCCS}$ | | 0.0 | 0.0 | 0.0 | 0.0 | 0.0 | 1.0 |
| $S_{PreCCS}$ | | 0.0 | 0.0 | 0.0 | 0.0 | 0.0 | 1.0 |
| $S_{PostEm}$ | | 1.0 | 1.0 | 1.0 | 1.0 | 1.0 | 0.0 |
| $S_{PreEm}$ | | 1.0 | 1.0 | 1.0 | 1.0 | 1.0 | 0.0 |

Figure 6: Optimal values of the operational decision variables for Case 2 (With Waste Tire tipping fees of 100 $/tonne). The corresponding economic results are in Figure 7. [1] $P_{Olefins}$ denotes the price of ethylene and propylene.

| **Case** | | S1 | S2 | S3 | S4 | S5 | S6 |
|---|---|---|---|---|---|---|---|
| **Capital costs** | | 0.0 | 0.0 | 0.0 | 0.0 | 0.0 | 0.0 |
| Waste tire train | | 0.0 | 0.0 | 0.0 | 0.0 | 0.0 | 0.0 |
| Gasifier | M$ | 268.8 | 278.7 | 215.4 | 278.7 | 215.4 | 278.7 |
| One train sulfur removal | M$ | 0.0 | 0.0 | 0.0 | 0.0 | 0.0 | 0.0 |
| Natural gas train | | 0.0 | 0.0 | 0.0 | 0.0 | 0.0 | 0.0 |
| Reformer | M$ | 18.3 | 0.0 | 53.6 | 0.0 | 35.4 | 0.0 |
| Liquified (Synthetic) NG train | | 0.0 | 0.0 | 0.0 | 0.0 | 0.0 | 0.0 |
| WGS 1 | M$ | 0.0 | 15.2 | 0.0 | 0.0 | 0.0 | 0.0 |
| Sulfur removal | M$ | 0.0 | 42.3 | 0.0 | 0.0 | 0.0 | 0.0 |
| $CO_2$ removal | M$ | 0.0 | 29.6 | 0.0 | 0.0 | 0.0 | 0.0 |
| Methanation | M$ | 0.0 | 55.3 | 0.0 | 0.0 | 0.0 | 0.0 |
| Liquefaction | M$ | 0.0 | 24.9 | 0.0 | 0.0 | 0.0 | 0.0 |
| Methanol train | M$ | 0.0 | 0.0 | 0.0 | 0.0 | 0.0 | 0.0 |
| WGS 2 | M$ | 9.7 | 0.0 | 9.7 | 15.2 | 9.7 | 15.2 |
| Sulfur removal | M$ | 42.3 | 0.0 | 27.9 | 42.3 | 27.9 | 42.3 |
| $CO_2$ removal | M$ | 31.8 | 0.0 | 19.6 | 31.8 | 19.6 | 31.8 |
| Methanol synthesis | M$ | 62.4 | 0.0 | 81.2 | 81.2 | 81.2 | 62.4 |
| DME synthesis | M$ | 0.0 | 0.0 | 0.0 | 100.5 | 0.0 | 0.0 |
| MTO | M$ | 0.0 | 0.0 | 0.0 | 0.0 | 206.8 | 0.0 |
| Power system | M$ | 110.2 | 70.9 | 110.2 | 110.2 | 110.2 | 110.2 |
| DGA | M$ | 0.0 | 0.0 | 0.0 | 0.0 | 0.0 | 31.3 |
| $CO_2$ compression & sequestration | M$ | 0.0 | 0.0 | 0.0 | 0.0 | 0.0 | 7.9 |
| ASU | M$ | 164.6 | 164.6 | 164.6 | 164.6 | 164.6 | 164.6 |
| Water systems | M$ | 47.6 | 29.3 | 63.2 | 63.2 | 63.2 | 63.2 |
| Miscellaneous | M$ | 52.6 | 52.6 | 52.6 | 52.6 | 52.6 | 52.6 |
| Total capital costs ($Cap$) | M$ | 808.3 | 763.4 | 798.0 | 940.3 | 986.6 | 860.2 |
| **Product portfolio** | | | | | | | |
| Liquefied SNG | kg/s | 0.0 | 10.2 (97.2%) | 0.0 | 0.0 | 0.0 | 0.0 |
| Electricity | MW | 48.0 (9.5%) | 13.9 (2.8%) | 17.4 (3.1%) | 14.8 (3.6%) | 47.6 (23.3%) | 27.7 (5.7%) |
| Methanol | kg/s | 21.8 (90.5%) | 0.0 | 25.5 (96.9%) | 0.0 | 0.0 | 21.5 (94.3%) |
| DME | kg/s | 0.0 | 0.0 | 0.0 | 13.4 (96.4%) | 0.0 | 0.0 |
| Ethylene | kg/s | 0.0 | 0.0 | 0.0 | 0.0 | 1.8 (41.1%) | 0.0 |
| Propylene | kg/s | 0.0 | 0.0 | 0.0 | 0.0 | 1.6 (35.6%) | 0.0 |
| **Thermodynamic performance** | | | | | | | |
| Total thermal output | MW | 507.9 | 503.5 | 555.5 | 417.7 | 204.1 | 482.4 |
| Thermal efficiency (LHV) | % | 56.9 | 56.4 | 62.2 | 46.8 | 22.9 | 54.0 |
| **Environmental performance** | | | | | | | |
| Direct $CO_2$ emissions | kg/s | 36.7 | 40.0 | 27.4 | 36.2 | 35.6 | 0.3 |
| $CO_2$ sequestered | kg/s | 0.0 | 0.0 | 0.0 | 0.0 | 0.0 | 37.4 |
| **Economic performance** | | | | | | | |
| Annual Net Profit ($Pro_{net}$) | M$/year | 197.1 | 196.6 | 268.2 | 237.4 | 190.4 | 188.5 |
| Net Present Value (NPV) | M$ | 752.1 | 788.2 | 1292.1 | 935.6 | 543.1 | 641.9 |
| Total wall time (ANTIGONE) | s | 16676 | 4369 | 1969 | 28257 | 7630 | 7347 |

Figure 7: Capital costs, Product portfolio, Thermodynamic, Environmental and Economic performance of the proposed concept for Case 2 (With Waste Tire tipping fees of 100 $/tonne) under the 6 scenarios studied.

## 4. Sensitivity Analysis

### *4.1. Price changes for electricity ($P_{Elec}$) and natural gas ($P_{NG}$) at 3 different methanol price ($P_{MeOH}$) points*

Figures 8, 9 and 10 present the influence of changes in $P_{Elec}$ and $P_{NG}$ on the primary product, NPV and mass of waste tire used in Case 1 (without tipping fees). We note that a global optimization problem is solved at each grid point. The graphs on left corresponds to a scenario in which the methanol price ($P_{MeOH}$) is fixed at $1\sigma$ below average, the middle graph corresponds to average $P_{MeOH}$, while the graphs on the right correspond to $P_{MeOH}$ fixed at $1\sigma$ above average. Analogous results for Case 2 (with tipping fees) are presented in Figures 11, 12 and 13. The results show that levying tipping fees allows for greater utilization of waste tire which in turn implies that designs that favor the production of methanol or DME are optimal for a wider range of product prices. Thus, the production of LNG (from natural gas or waste tire) occurs in fewer price scenarios if tipping fees are implemented.

### *4.2. Price changes for methanol ($P_{MeOH}$) and DME ($P_{DME}$)*

Figures 14, 15, 16 present the influence of changes in ($P_{MeOH}$) and DME ($P_{DME}$) on the primary product, NPV and waste tire flow rates for Case 1 (without tipping fees) with analogous results for Case 2 (with tipping fees) presented in Figures 17, 18, 19. Similar to the previous section, the imposition of waste tire tipping fees results in an increase in the proportion of tire used. Consequently, for Case 2, the production of methanol or DME is favored for a wider range of price points compared to Case 1 as this mode allows for the exploitation of synergies gained by co-utlization of waste tire and natural gas.

### *4.3. Changes in $CO_2$ tax rates ($P_{CO_2}$)*

Figures 20 and 21 present the variation of $CO_2$ sequestered, $CO_2$ emitted, NPV, waste tire flow rate and mass flow rate of products with increasing $CO_2$ taxes from S1 (historically average prices) for Case 1 and Case 2 respectively. For Case 1, levying $CO_2$ taxes results in a switch in the primary product from electricity to methanol. In general, pre-combustion $CO_2$ capture is implemented at lower tax rates. On the other hand, post-combustion $CO_2$ capture requires higher tax rates. Implementing CCS in both cases results in a drop in NPV.

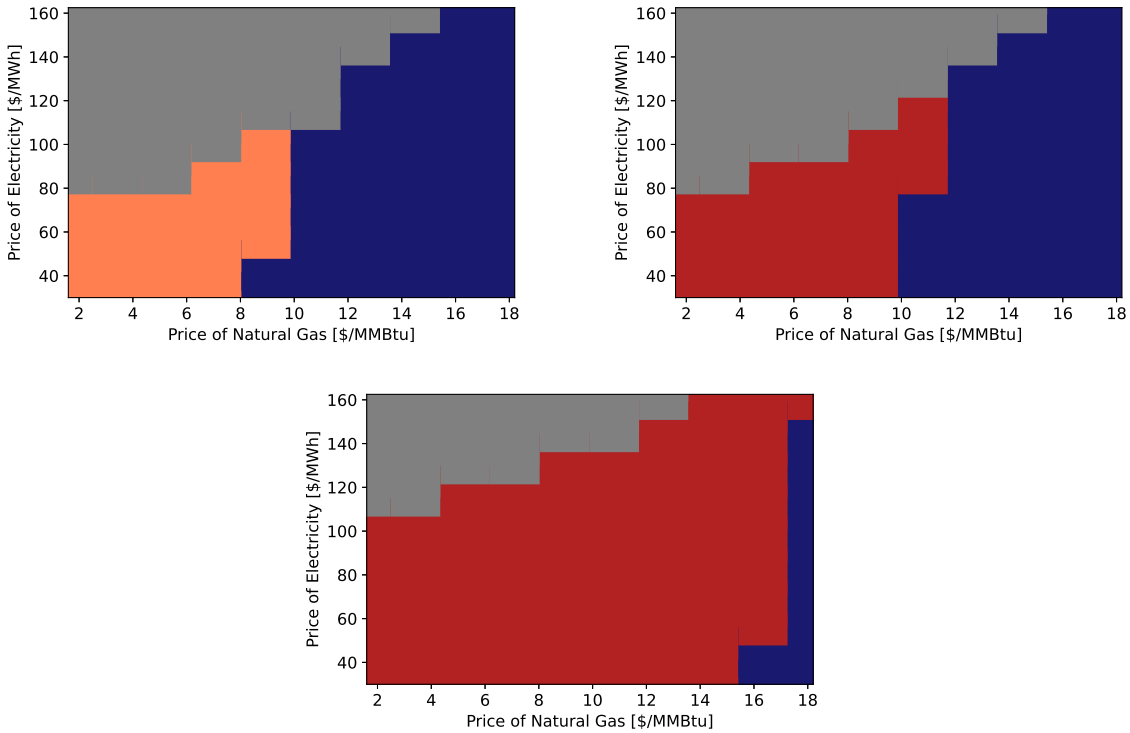


Figure 8: The optimal product portfolio for a variety of natural gas and electricity prices in Case 1 (without tipping fees) for low (left), average (middle) and high (right) methanol prices. Primary products: : DME, : Electricity, : Methanol, : Liquefied SNG, :Olefins

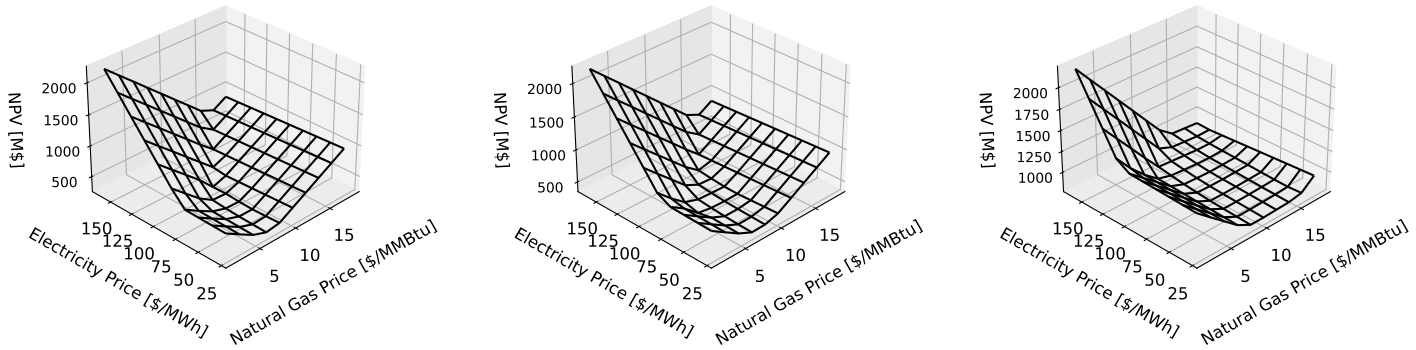


Figure 9: Net Present Values corresponding to the optimal designs presented in Figure 8



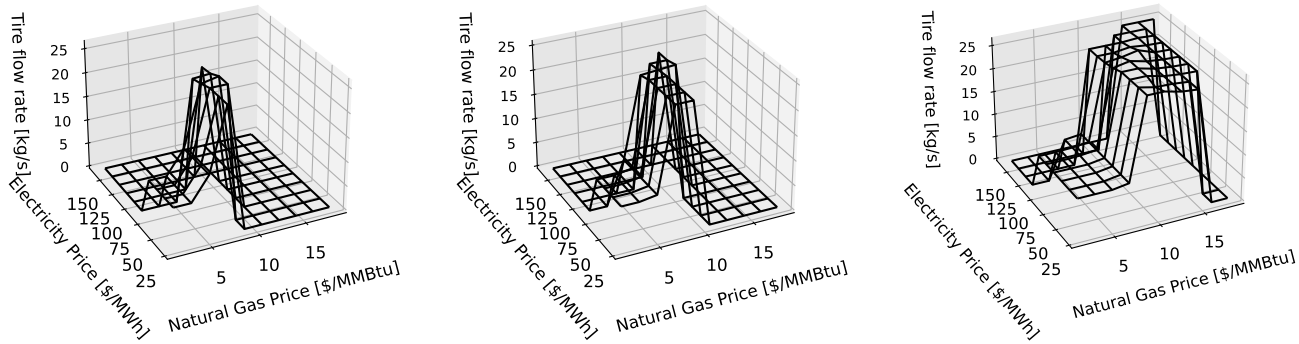


Figure 10: Tire mass flow rates for the optimal designs presented in Figure 8

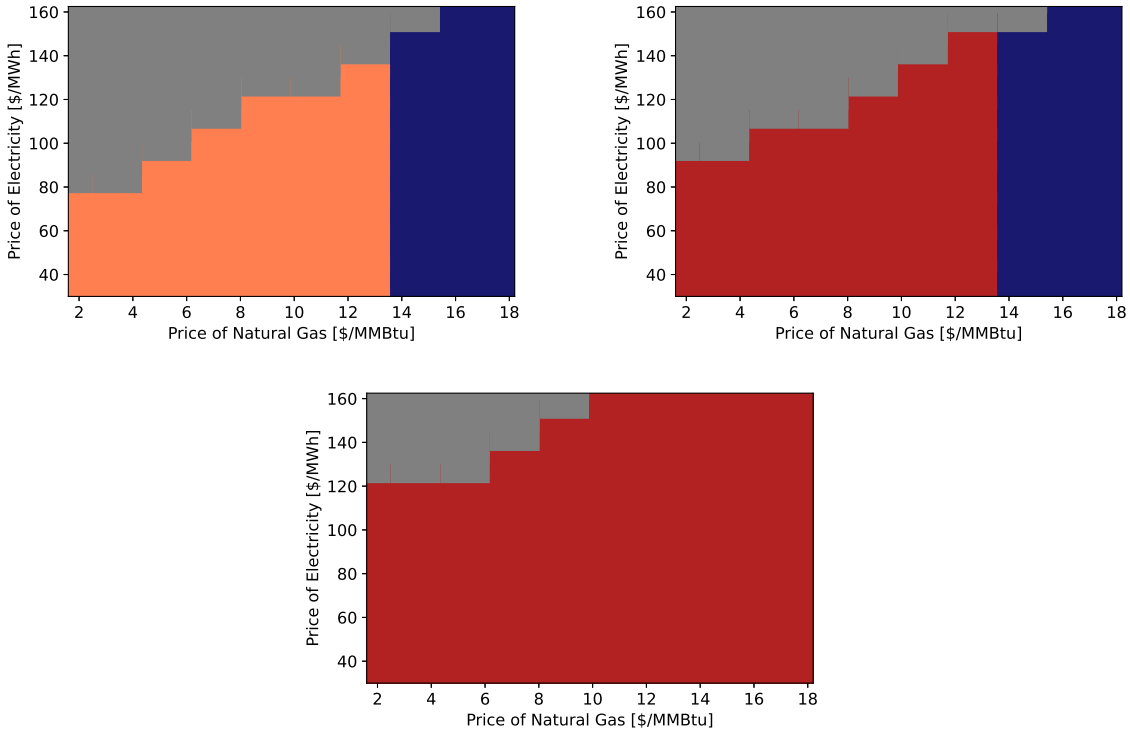


Figure 11: The optimal product portfolio for a variety of natural gas and electricity prices in Case 2 (with tipping fees of 100 $/tonne) for low (left), average (middle) and high (right) methanol prices. Primary products: : DME, : Electricity, : Methanol, : Liquefied SNG, :Olefins

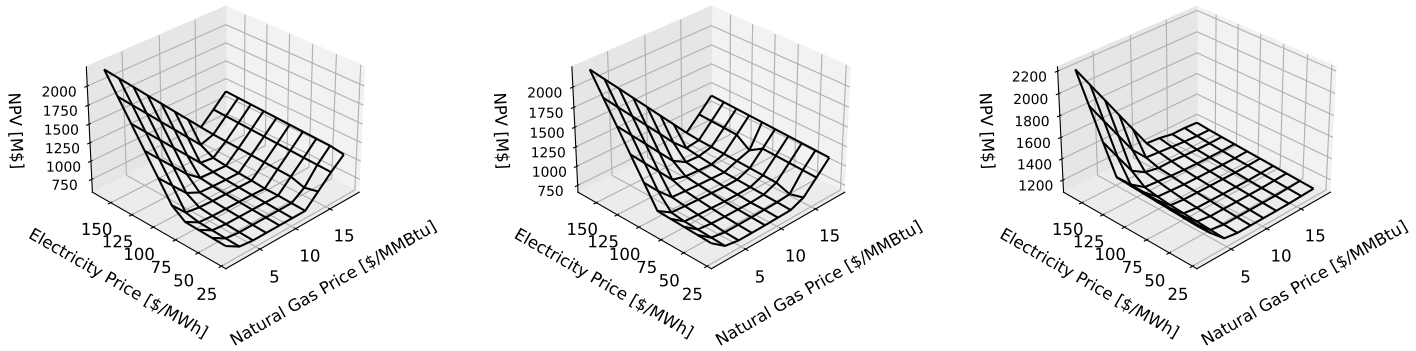


Figure 12: Net Present Values corresponding to the optimal designs presented in Figure 11



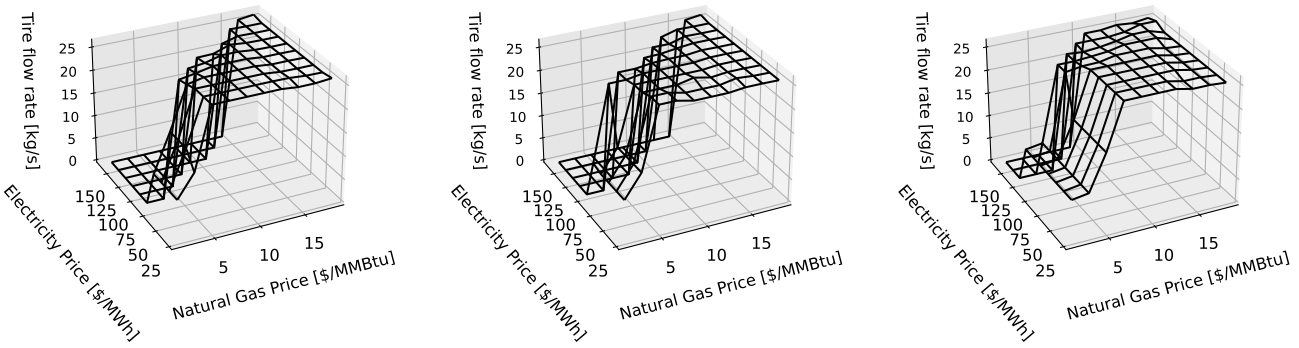


Figure 13: Tire mass flow rates for the optimal designs presented in Figure 11

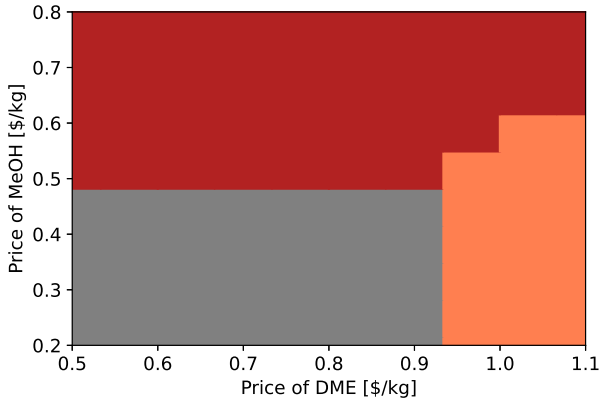


Figure 14: The optimal product portfolio for a variety of MeOH and DME prices for Case 1 (Without tipping fees). Primary products: : DME, : Electricity, : Methanol, : Liquefied SNG, :Olefins

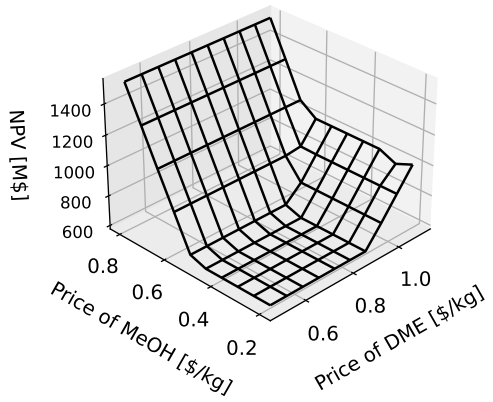


Figure 15: Net Present Values corresponding to the optimal designs presented in Figure 14

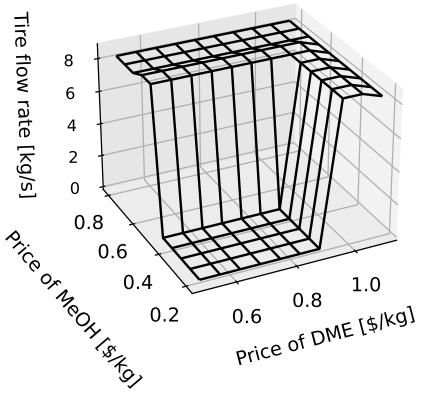


Figure 16: Tire mass flow rates for the optimal designs presented in Figure 14

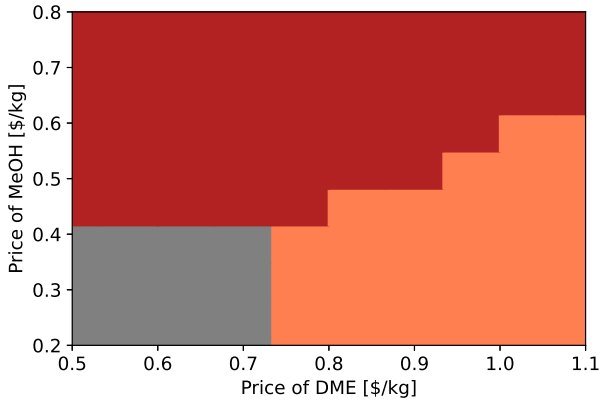


Figure 17: The optimal product choice for a range of MeOH and DME prices for Case 1 (With tipping fees of 100 $/tonne). Primary products: : DME, : Electricity, : Methanol, : Liquefied SNG, :Olefins

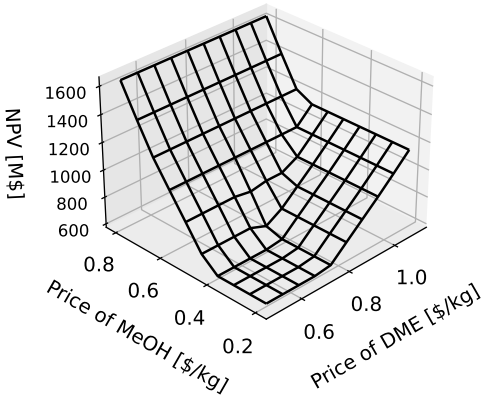


Figure 18: Net Present Values attained for the optimal designs presented in Figure 17

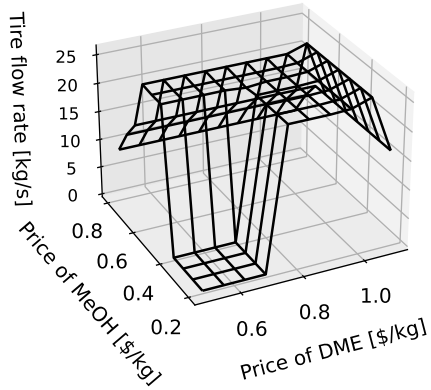


Figure 19: Tire mass flow rates for the optimal designs presented in Figure 17

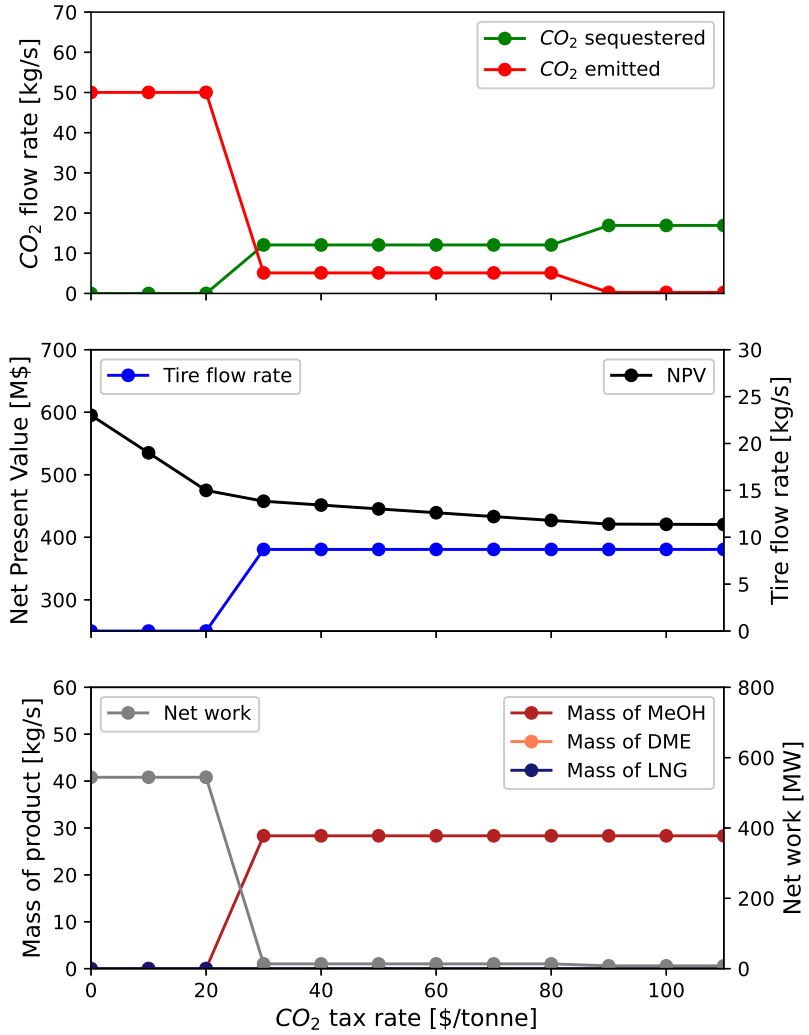


Figure 20: Variation of $CO_2$ sequestered, $CO_2$ emitted, Net Present Value, waste tire flow rates and Mass of products with increasing $P_{CO_2}$ for Case 1

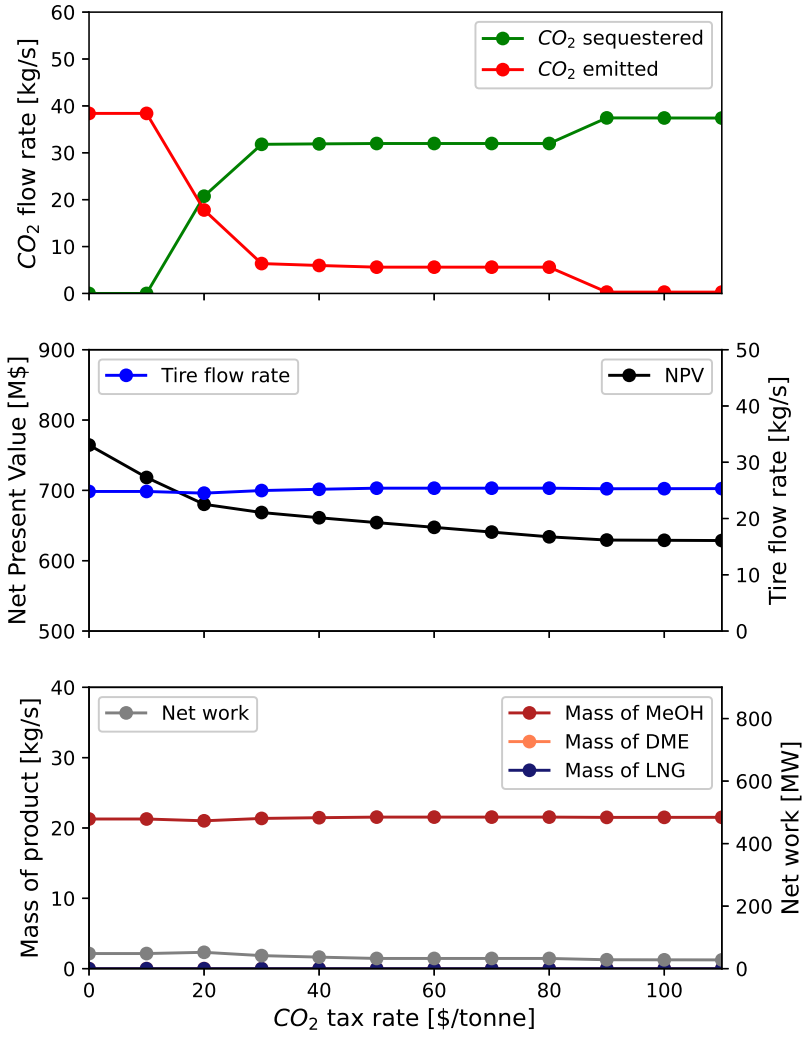


Figure 21: Variation of $CO_2$ sequestered, $CO_2$ emitted, Net Present Value, waste tire flow rates and Mass of products with increasing $P_{CO_2}$ for Case 2

## 5. Conclusions

The optimal design and operation of a novel process that converts a hybrid waste tire and natural gas feedstock to multiple products (electricity, methanol, dimethyl ether, liquefied natural gas, and olefins) is presented. The variation of the product portfolio with changing market conditions is investigated for two cases: Without and with waste tire tipping fees of 100 $/tonne. Several designs that exploit the synergies between the tire and natural gas conversion trains for the production of methanol or DME are presented. In addition, a sensitivity analysis is performed to study the variation of design and operating conditions with changing prices. In general, the results suggest that a greater quantity of waste tire is utilized when tipping fees are levied which in turn results in the production of methanol or DME in a wider range of market conditions as a result of efficiency gains due to exploitation of certain synergies.

However, we note that the optimal product portfolio is highly sensitive to the prevailaing market conditions. This motivates our follow-up work on the design under uncertainty of flexible polygeneration processes (using a two-stage stochastic programming approach) that are able to adjust operating conditions in response to changing prices.

## Acknowledgements

We thank Flemming Holtorf of MIT, Rohit Kannan of the Center for Nonlinear Studies and Theoretical Division (Los Alamos National Laboratory) for helpful discussions. The first author gratefully acknowledges the financial support from NTNU's Department of Energy and Process Engineering and from NTNU Energy. This publication has been funded by HighEFF - Centre for an Energy-Efficient and Competitive Industry for the Future. The authors gratefully acknowledge the financial support from the Research Council of Norway and user partners of HighEFF, an 8-years Research Centre under the FME-scheme (Centre for Environment-friendly Energy Research, 257632). We also acknowledge support from the McMaster Advanced Control Consortium for use of the multi-core computer.

## Conflicts of Interest

The authors declare no conflicts of interest.

## References


[1] K. Farhat, S. Reichelstein, Economic value of flexible hydrogen-based polygeneration energy systems, Applied Energy 164 (2016) 857–870.

[2] C. A. Floudas, J. A. Elia, R. C. Baliban, Hybrid and single feedstock energy processes for liquid transportation fuels: a critical review, Computers & Chemical Engineering 41 (2012) 24–51.

[3] T. A. Adams II, P. I. Barton, Combining coal gasification and natural gas reforming for efficient polygeneration, Fuel Processing Technology 92 (2011) 639–655.

[4] L. Hoseinzade, T. A. Adams II, Techno-economic and environmental analyses of a novel, sustainable process for production of liquid fuels using helium heat transfer, Applied Energy 236 (2019) 850–866.

[5] Y. K. Salkuyeh, T. A. Adams II, Combining coal gasification, natural gas reforming, and external carbonless heat for efficient production of gasoline and diesel with CO2 capture and sequestration, Energy Conversion and Management 74 (2013) 492–504.

[6] A. S. R. Subramanian, T. Gundersen, T. A. Adams II, Technoeconomic analysis of a waste tire to liquefied synthetic natural gas (SNG) energy system, Energy (2020) 117830.

[7] A. S. R. Subramanian, T. Gundersen, T. A. Adams II, Optimal design and operation of a waste tire feedstock polygeneration system, Energy (2021) 11990.

[8] A. M. Niziolek, O. Onel, M. F. Hasan, C. A. Floudas, Municipal solid waste to liquid transportation fuels–Part II: Process synthesis and global optimization strategies, Computers & Chemical Engineering 74 (2015) 184–203.

[9] I. J. Okeke, T. A. Adams II, Combining petroleum coke and natural gas for efficient liquid fuels production, Energy 163 (2018) 426–442.

[10] Y. K. Salkuyeh, T. A. Adams II, Integrated petroleum coke and natural gas polygeneration process with zero carbon emissions, Energy 91 (2015) 479–490.

[11] Y. Chen, T. A. Adams II, P. I. Barton, Optimal design and operation of static energy polygeneration systems, Industrial & Engineering Chemistry Research 50 (2010) 5099–5113.

[12] T. A. Adams II, J. H. Ghouse, Polygeneration of fuels and chemicals, Current Opinion in Chemical Engineering 10 (2015) 87–93.

[13] K. Jana, A. Ray, M. M. Majoumerd, M. Assadi, S. De, Polygeneration as a future sustainable energy solution - A comprehensive review, Applied Energy 202 (2017) 88–111.

[14] S. Murugan, B. Horak, Tri and polygeneration systems - A review, Renewable and Sustainable Energy Reviews 60 (2016) 1032–1051.

[15] E. D. Larson, H. Jin, F. E. Celik, Large-scale gasification-based coproduction of fuels and electricity from switchgrass, Biofuels, Bioproducts and Biorefining 3 (2009) 174–194.

[16] H. Boerrigter, A. Van Der Drift, Biosyngas: Description of R&D trajectory necessary to reach large-scale implementation of renewable syngas from biomass, Energy research Centre of the Netherlands (2004).

[17] L. Hoseinzade, T. A. Adams, Dynamic modeling of integrated mixed reforming and carbonless heat systems, Industrial & Engineering Chemistry Research 57 (2017) 6013–6023.

[18] A. S. R. Subramanian, R. Kannan, F. Holtorf, T. A. Adams II, T. Gundersen, P. I. Barton, Optimization under uncertainty of a hybrid waste tire and natural gas feedstock flexible polygeneration system using a decomposition algorithm, Pre-print available at http://psecommunity.org/LAPSE:2021.0798 (2022).

[19] A. S. R. Subramanian, T. A. Adams II, T. Gundersen, P. I. Barton, Optimal Design and Operation of Flexible Polygeneration Systems using Decomposition Algorithms, in: Computer Aided Chemical Engineering, volume 48, Elsevier, 2020, pp. 919–924.

[20] J. Meerman, A. Ramırez, W. Turkenburg, A. Faaij, Performance of simulated flexible integrated gasification polygeneration facilities. Part A: A technical-energetic assessment, Renewable and Sustainable Energy Reviews 15 (2011) 2563–2587.

[21] J. Meerman, A. Ramırez, W. Turkenburg, A. Faaij, Performance of simulated flexible integrated gasification polygeneration facilities, Part B: Economic evaluation, Renewable and Sustainable Energy Reviews 16 (2012) 6083–6102.

[22] M. Martín, I. E. Grossmann, Optimal use of hybrid feedstock, switchgrass and shale gas for the simultaneous production of hydrogen and liquid fuels, Energy 55 (2013) 378–391.

[23] J. E. Santibañez-Aguilar, J. B. González-Campos, J. M. Ponce-Ortega, M. Serna-González, M. M. El-Halwagi, Optimal planning and site selection for distributed multiproduct biorefineries involving economic, environmental and social objectives, Journal of cleaner production 65 (2014) 270–294.

[24] Y. Chen, T. A. Adams II, P. I. Barton, Optimal design and operation of flexible energy polygeneration systems, Industrial & Engineering Chemistry Research 50 (2011) 4553–4566.

[25] R. C. Baliban, J. A. Elia, C. A. Floudas, Optimization framework for the simultaneous process synthesis, heat and power integration of a thermochemical hybrid biomass, coal, and natural gas facility, Computers & Chemical Engineering 35 (2011) 1647–1690.

[26] A. Cozad, N. V. Sahinidis, D. C. Miller, Learning surrogate models for simulation-based optimization, AIChE Journal 60 (2014) 2211–2227.

[27] Z. T. Wilson, N. V. Sahinidis, The ALAMO approach to machine learning, Computers & Chemical Engineering 106 (2017) 785–795.

[28] R. Kannan, Algorithms, analysis and software for the global optimization of two-stage stochastic programs, Ph.D. thesis, Massachusetts Institute of Technology, 2017.

[29] R. Misener, C. A. Floudas, ANTIGONE: Algorithms for Continuous/Integer Global Optimization of Nonlinear Equations, Journal of Global Optimization 59 (2014) 503–526.

[30] X. Li, A. Sundaramoorthy, P. I. Barton, Nonconvex Generalized Benders Decomposition, in: Optimization in Science and Engineering, Springer, 2014, pp. 307–331.

[31] X. Li, A. Tomasgard, P. I. Barton, Nonconvex Generalized Benders Decomposition for stochastic separable mixed-integer nonlinear programs, Journal of Optimization Theory and Applications 151 (2011) 425.

[32] M. C. Woods, P. Capicotto, J. L. Haslbeck, N. J. Kuehn, M. Matuszewski, L. L. Pinkerton, M. D. Rutkowski, R. L. Schoff, V. Vaysman, Cost and performance baseline for fossil energy plants, National Energy Technology Laboratory (2007).

[33] C. Kunze, H. Spliethoff, Modelling, comparison and operation experiences of entrained flow gasifier, Energy Conversion and Management 52 (2011) 2135–2141.

[34] W. D. Seider, J. D. Seader, D. R. Lewin, Product & Process Design Principles: Synthesis, Analysis and Evaluation, John Wiley & Sons, 2009.

[35] U.S. Energy Information Administration. Natural Gas Prices., `https://www.eia.gov/dnav/ng/ng_pri_sum_dcu_nus_m.htm`, 2020. [Online; accessed 11-June-2020].

[36] K. Jordal, P. A. M. Ystad, R. Anantharaman, A. Chikukwa, O. Bolland, Design-point and part-load considerations for natural gas combined cycle plants with post combustion capture, International Journal of Greenhouse Gas Control 11 (2012) 271–282.

[37] Y. Salkuyeh, T. A. Adams II, Co-production of olefins, fuels, and electricity from conventional pipeline gas and shale gas with near-zero CO2 emissions. Part I: process development and technical performance, Energies 8 (2015) 3739–3761.